Squeezing Flows of Polymeric Liquids

ROGER J. GRIMM

Department of Chemical Engineering
and Rheology Research Center
University of Wisconsin
Madison, Wisconsin 53706

An experimental study has been done on the flow of viscoelastic liquids squeezed between two flat parallel plates. In fast squeezes under a constant load, the plates did not come together as rapidly as predicted by inelastic fluid theory. Our experimental data suggest that this device is not generally useful as a viscometer.

SCOPE

Squeezing types of flows are encountered in many industrial systems, from plastics molding operations to lubricated bearings. They are produced by the action of a force normal to two parallel plates with fluid in between (see Figure 1). In this paper, we report on an extensive experimental study on squeezing flows of polymeric liquids. The experiments involved applying a step-function force to circular plates and observing the decrease in distance between the plates as a function of time (Figure 2).

At least three objectives can be cited for this work:

1. Determination of the limits of applicability of theories that ignore the elastic properties of polymeric liquids. Devices incorporating the squeeze flow geometry in their design have been used in industry for many years, primarily for quality control tests on such materials as asphalts and rubbers. They are known by several names, including parallel plate plastometers, parallel plate viscometers, transverse flow viscometers, and compression plastometers. It would be useful to determine if these devices may be used as viscometers for non-Newtonian fluids. To do so we need to determine under what experimental conditions various theoretical expressions apply.

2. Provision of data for evaluation of constitutive equations and for evaluation of methods of solving hydrodynamics problems. One of the ongoing goals of rheologists is to develop better constitutive equations and better techniques for solving hydrodynamics problems. Squeezing flows provide a good testing ground for theories, since the flow pattern is simple but nontrivial.

3. Provision of information related to polymer processing and to lubrication. As mentioned earlier, squeezing flows are encountered in many industrial operations. An improved understanding of the flow should provide information that is at least qualitatively useful for design.

Furthering work towards these objectives, two recent experimental studies have been reported on polymeric liquids, one by Leider (1974) and the other by Brindley, Davies, and Walters (1976). Both correlated their results in terms of a half time for each experiment, defined as the time for half of the fluid that is initially in the gap to be squeezed out. They found that for slow squeezes, the theories that ignored elastic properties adequately modeled the flow. In fast squeezes, however, the top plate descended much more slowly than predicted by theory.

In our work we have carried out an extensive experimental program to determine whether the trend observed by these earlier workers holds for a large set of polymeric liquids. Since the faster squeezes seemed to be of most interest, we have tried to emphasize these. Complete curves of plate separation vs. time will be presented for our data, providing more information than is contained in only the half time measurement. We also have done a limited flow visualization study to check for the presence of secondary flows.

CONCLUSIONS AND SIGNIFICANCE

Our data on polymer solutions follows the pattern observed by Leider (1974) and by Brindley, Davies, and Walters (1976). That is to say, the inelastic fluid theories predicted slow squeeze behavior well, but failed for fast squeezes.

Most of the slower experiments could be modeled only by using the complete viscosity vs. shear rate curve, however, and the power law equation was not usually adequate. This implies that we cannot use the slow squeeze data to obtain power law constants for liquids in general, although occasionally one may be able to do so (Leider, 1974). Since at the present time no technique has been developed for obtaining the complete viscosity curve from squeezing flow data, we must conclude that a squeezing flow device cannot be used as a viscometer.

In the fast squeezes the top plate approached the lower plate more slowly than predicted by the inelastic fluid theories. This is in marked contrast to the predictions of several equations that have been derived for viscoelastic liquids (Tanner, 1965; Kramer, 1974; Brindley et al., 1976). It implies that polymer solutions are better lubricants than would be predicted from the theories. Furthermore, the complete curves of plate separation as a function of time show a distinctive S shape, in contrast to other theoretical predictions (Parlato, 1969; Leider and Bird, 1974). (The S shape is not a result of either apparatus or fluid inertia, although they would produce such a shape.) The lack of agreement between the experimental data and the theories is probably due to a combination of the constitutive equations that are used and the assumptions that are made regarding the kinematics of the flow. Our flow visualization experiments did not reveal any secondary flows that might complicate mathematical analysis.

A correlation of the data on the polymer solutions has been developed, and is presented in Figures 12 and 13. For complete data on all of the fluids, the reader is referred to the thesis by Grimm (1977).

Roger J. Grimm is with Amoco Chemicals Corporation, Naperville, Illinois 60540.

0001-1541-78-1024-0427-$01.55.

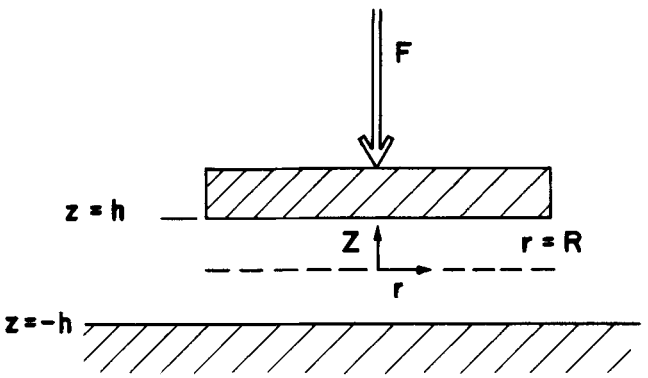

Fig. 1. Squeeze film geometry. The fluid rests in the gap between the plates. In practice the ratio R/h was of the order of 100.

SURVEY OF PREVIOUS WORK

Theoretical Studies

The first mathematical study to be carried out was done in 1874, by Stefan, who analyzed the flow for Newtonian liquids. In 1931 Scott extended the analysis to include power law fluids, that is, fluids that have a constitutive equation of the form

$$\underline{\tau} = -m\left|\sqrt{\tfrac{1}{2}\left(\underline{\dot{\gamma}} : \underline{\dot{\gamma}}\right)}\right|^{n-1}\underline{\dot{\gamma}} \qquad (1)$$

Scott's development led to

$$F = \frac{(-\dot{h})^n}{h^{2n+1}}\left(\frac{2n+1}{2n}\right)^n \frac{\pi m R^{n+3}}{n+3} \qquad (2)$$

By treating Equation (2) as a differential equation in h, and by considering F to be constant F_0, we obtain the following expression for plate separation as a function of time:

$$h = \left[h_0^{-(1+1/n)} + \left(1+\frac{1}{n}\right)kt\right]^{\frac{-n}{1+n}} \qquad (3)$$

where

$$k = \left[\frac{F_0}{\pi m R^{n+3}}\left(\frac{2n}{2n+1}\right)^n (n+3)\right]^{1/n} \qquad (4)$$

Since complete developments of Equation (2) are given elsewhere (Scott, 1931; Na, 1966; Leider and Bird, 1974; Bird et al., 1977), the derivation will not be repeated here.

Since the time of Scott, a number of authors have modeled the flow using other constitutive equations. A good review of many of their theories is given by Leider and Bird (1974). We have attempted to summarize the salient points of the developments in Table 1. Plots of predicted plate separation as a function of time for these theories are included later in this paper, where the experimental data will be presented and discussed.

Experimental Studies

Before discussing experimental studies on viscoelastic fluids, we must first define a Deborah number *De*. A Deborah number is a ratio of a characteristic time for the material λ to a characteristic time for the experiment. Usually, when *De* is large, the material is observed to behave elastically, and when *De* is small, the material behaves as if it were purely viscous. In our case, we will take

$$De = \lambda/t_{1/2} \qquad (5)$$

where $t_{1/2}$ is the half time defined in Figure 2. When *De* is less than unity in a given experiment, the fluid can be said to have been squeezed slowly. When *De* is greater than unity, the fluid can be said to have been subjected to a fast squeeze. The characteristic time for a material may be defined in any of several ways, most of which give approximately the same number. In our work we will define

$$\lambda = (m/\eta_0)^{1/(n-1)} \qquad (6)$$

where η_0 is the zero shear rate viscosity, because this definition permits us to obtain λ from measurements of viscosity alone.

Of the many authors who have studied viscoelastic fluids in the plastometer, perhaps the first was Dienes (1947) (also see Dienes and Klemm, 1946). He used his apparatus to measure stress relaxation and to do recovery experiments, as well as to do the more traditional squeezing experiments. Unfortunately, by his own admission, his tests were not very accurate, and his analysis was oversimplified by the assumption of linear viscoelasticity.

Recently, several attempts have been made to observe the behavior of polymer solutions subjected to fast squeezes (Parlato, 1969; Hirst and Lewis, 1973; Leider, 1974; Brindley et al., 1976; Binding et al., 1976). The paper by Leider warrants some special discussion, since it was largely in response to his interesting findings that the present work was begun. Leider's study was the first systematic investigation of its kind, in which experiments were done on both Newtonian and viscoelastic liquids and the results compared with independently determined viscosities. He found that in the slower squeezes the Scott equation, Equation (2), was followed quite closely, but that in the faster squeezes the data deviated greatly from the Scott prediction. In these fast squeezes the plates did not come together as quickly as predicted from the Scott result. Leider estimated experimental half times from power law constants and a time constant for the given fluid. He also indicated a technique whereby a squeezing flow instrument could be used as a viscometer.

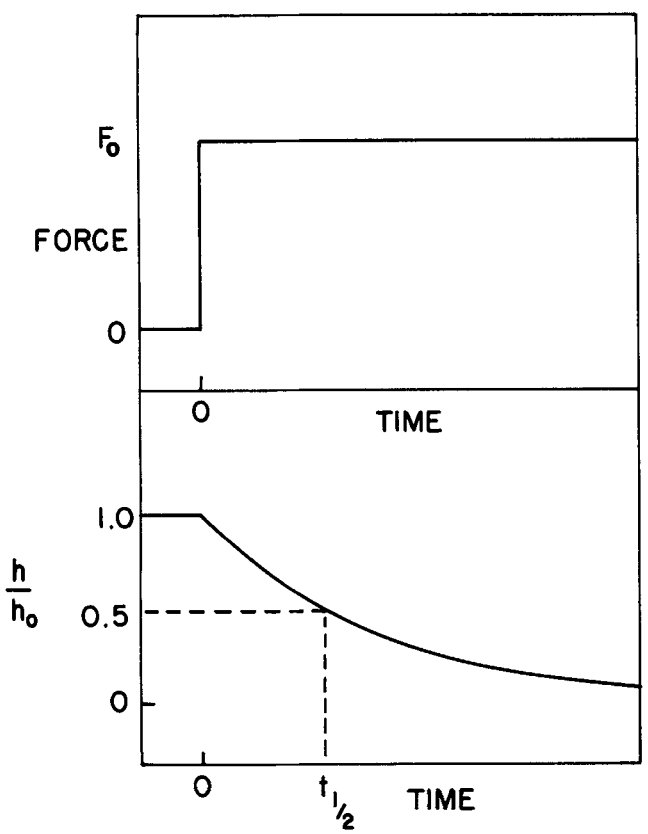

Fig. 2. Step function force usually used in experiment, and typical response of the plates. The gap height h is as defined in Figure 1.

TABLE 1. SOLUTIONS TO SQUEEZE FLOW PROBLEM FOR PARALLEL CIRCULAR DISKS

Year	Investigators	Fluid model	Stress overshoot predicted by model?*	Properties of model and assumptions	Predicted half time greater or less than Scott half time?†	Remarks
1874	Stefan	Newtonian	No		Same when $n = 1$	Fits Newtonian data well
1931	Scott	Power law	No		Same	
1965	Tanner	Convected Maxwell model with power law viscosity	No	Neglects normal stresses	Less	
1969	Parlato (see also Metzner, 1971)	Convected Maxwell model with constant viscosity	No	Assumes flow is primarily elongational (EPF approximation); this assumption is criticized by Williams and Tanner, 1970)	Greater	
1974	Kramer	Lodge rubberlike liquid	No	Uses only one exponential term in the memory function; model does not predict shear rate dependent viscosity	Less	Numerical work was done
1974	Leider and Bird	Power law fluid with an empirical overshoot correction factor included	Yes	Rough estimation according to authors	Greater	Authors conclude model must be able to predict stress overshoot
1974	Co and Bird	Goddard-Miller model	Yes, followed by oscillations	Assumes power law velocity profiles; neglects normal stresses	Same**	Numerical work was done
1976	Brindley, Davies, and Walters	Inelastic fluid with arbitrary viscosity vs. shear rate function	No			Numerical work was done
1976	Brindley, Davies, and Walters	Second-order fluid	No	Model does not predict shear rate dependent viscosity; perturbation approach used	Less	We conclude that normal stresses are not cause of high De experimental behavior

* Shear stress overshoot at the inception of a simple shear flow.

† The half time $t_{1/2}$ is defined in Figure 2. The question asked here is whether the given theory predicts a half time greater than or less than the prediction of the Scott equation [Equation (24)] for high Deborah number flows or fast squeezes. Experimentally, in fast squeezes, the half time has been found to be greater than the Scott half time.

** Low Deborah number calculation only.

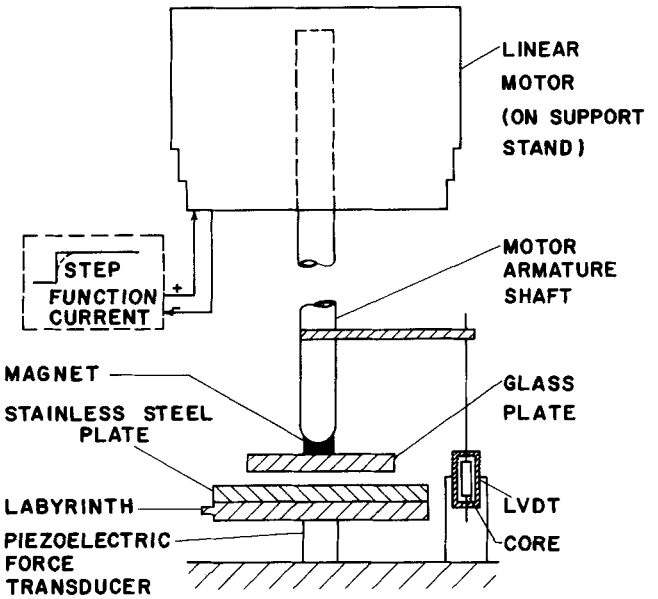

Fig. 3. Schematic diagram of squeezing flow apparatus.

Brindley, Davies, and Walters carried out a study similar to the one performed by Leider. Once again, they presented their results primarily in terms of half time measurements, although they did present a few complete curves of distance between plates as a function of time to illustrate a bouncing behavior that they observed. In some of their fastest experiments, the top plate bounced and did not descend smoothly with time. A half time measurement was thus recognized as not being sufficient to characterize the flow behavior. Brindley, Davies, and Walters reached essentially the same conclusions regarding the Scott prediction that Leider made, but made two additional observations.

1. The zero shear rate viscosity region extended to rather large shear rates for one of their fluids, resulting in errors when the Scott power law equation was used for slow squeezes. The authors developed a computer technique for use with an arbitrary viscosity-shear rate profile and found that its predictions fit the data extremely well. Their observation, however, indicates that caution must be used in using a squeezing flow instrument as a viscometer.

2. In some of their faster squeezes, the inertia of the weight used to provide the force F needed to be considered. This could be done in a rather straightforward way, although use of a computer was necessary.

EXPERIMENTAL

Squeezing Flow Apparatus

A schematic diagram of the apparatus is shown in Figure 3. Force was applied to the plates by the linear motor shown at the top of the figure. Since one of our goals was to do fast experiments, with half times as small as 50 ms, we were concerned about the inertia of the apparatus. Use of a motor with a low mass armature allowed us to apply relatively large forces with minimal inertial problems. More consideration will be given to the question of inertia later.

To obtain a step function force, it was necessary to apply a step function current to the motor. The force was measured and checked for vibration with a piezoelectric force transducer located beneath the lower plate. Since piezoelectric transducers are suitable only for dynamic measurements, it was not possible to verify that the force was constant over long time periods with this device, but the transducer did prove particularly useful in measuring the rise time of the force. It was found that a minimum rise time constant of 2 ms was required, since if the force was applied more quickly, significant vibration of the apparatus resulted.

The distance between the plates was measured with a linear variable differential transformer (LVDT). The coil of the transducer was mounted firmly to the base of the apparatus, whereas the transducer core moved up and down with the plunger, and hence the top plate. It is estimated that the gap measurements could be made with an accuracy of $\pm 2\%$.

Since the viscosity of most polymeric liquids is highly temperature dependent, it was necessary to have some type of temperature control system. Fortunately, the gap between the plates was always quite small, so that it was sufficient to control the temperature of only the lower plate. This was accomplished by circulating water from a temperature bath in a labyrinth beneath the lower plate, which was made of stainless steel. All experiments were run at 25 ± 0.1°C.

The upper plate was made of glass and was attached by means of a spherically hollowed out magnet to a ball bearing on the end of the motor armature shaft. This essentially one-point contact caused the top plate to descend parallel to the lower plate. Complicated procedures for aligning the two plates were thus eliminated. Both the top and the bottom plate could be easily removed for cleaning. Five different upper plates were used, with diameters ranging from 0.9525 to 5.080 ± 0.005 cm.

Data Recording System

Since we wished to do a large number of experiments, it was apparent that a considerable amount of repetitive data reduction would be required. As a first step we decided to digitize the complete h (t) curve using analogue to digital (A/D) converters on a minicomputer available to us. The minicomputer was not located in our laboratory, so during experimentation we stored the output voltage signal from the LVDT temporarily on a Telex FM tape recorder. The tape recorder was then transported to the room containing the PDP-11/40 minicomputer, where we could process the signal at our convenience. Once digitized, the data could be easily transferred to a larger computer for further data analysis.

Experimental Design

A factorial design on the variables F, R, and h_0 was run on each of the fluids within the following constraints:

1. Two force levels, two initial gaps h_0, and five plates of different radius were used. Since h_0 could be measured more accurately than it could be preset, that dimension of the factorial design contained some variability.
2. The aspect ratio R/h_0 was kept greater than 50 for all fluids except the Silly Putty®, for which the ratio went as low as 10.
3. Very few experiments were run for which the half time was less than 50 ms.

FLUIDS

Seven different fluids were tested in this study. Table 2 summarizes the viscosity data for these fluids.

Power law constants for all of the fluids except for the Silly Putty® were determined using a Ferranti-Shirley cone-and-plate viscometer. The shear rate range covered usually was between 85 s^{-1} and about 5 000 s^{-1}, with the upper bound being limited by the angular velocity of the cone at which the fluid spun out of the gap. Generally, the maximum shear rate obtained with the Ferranti-Shirley was lower than the maximum shear rates in the fastest squeezing flow experiments. The estimated error (repeatability) of the measurements made with the Ferranti-Shirley was about $\pm 3\%$.

Zero shear rate viscosities were determined for the HEC and PA solutions with a falling ball viscometer. A description of the technique used to extrapolate to zero shear is given by Riddle, Narvaez, and Bird (1977) and follows the method outlined by Sutterby (1973). Unfortunately, our samples of PEO and of the latex suspension were too small to attempt falling ball measurements on them.

A third instrument was also used to measure the viscos-

TABLE 2. FLUIDS TESTED

Fluid	Power law constants [see Equation (1)] (Ferranti-Shirley viscometer) m (Pa·s^n)	n	Zero shear rate viscosity (Pa · s) (Falling-Ball viscometer)	Time constant, λ (s)
1) Mineral oil (Cannon Instrument Co. S600)	1.342	1.0	—	0
2) Polybutene (Cannon Instrument Co. S8000)	19.943	1.0	—	—
3) 0.9% hydroxyethyl cellulose (HEC) in a 50/50 glycerine/water mixture	14.5	0.395	9.90	0.534*
4) 3% polyacrylamide (PA) in a 60/40 glycerine/water mixture	14.1	0.482	50.5	11.7*
5) Silly Putty®	5.58×10^{4}**	0.781**	—	8.78×10^{-3}†
6) 2.5% polyethylene oxide (PEO), in water, with a small amount of isopropanol added as a preservative††	27.8	0.307	—	4‡
7) A 0.0842 volume fraction suspension of monodisperse polystyrene spheres ($d = 0.147$ μm) in fluid No. 6††	30.5	0.304	—	4‡

* Obtained from the intersection of the power law and the zero shear rate asymptotes. [See Equation (6).]
** From Weissenberg rheogoniometer.
† From normal stress measurements. $m' = 2.35 \times 10^5$, $n' = 1.11$, $\lambda = \left(\frac{m'}{2m}\right)^{\frac{1}{n'-n}}$
†† These fluids contained a high concentration of small air bubbles.
‡ Crude estimation from data of Turian (1964); also can be estimated from data of Novotny et al. (1973) using definition in (†). We have assumed that the latex particles did not alter the time constant of the PEO.

ity of the HEC solution. This was a stressmeter Mark III, designed by Professor A. S. Lodge and soon to be marketed by Seiscor Company, Tulsa, Oklahoma. Viscosities are determined from the pressure drop as the fluid flows through a narrow slit. Normal stress differences can be inferred from hole-pressure errors measured by the device (Higashitani and Lodge, 1975). The instrument we used was in the developmental stage, so that errors were rather large, but the viscosity measurements were useful in filling in the gap between the zero shear rate region and the power law region.

A plot of viscosity as a function of shear rate is given in Figure 4 for the HEC showing a comparison of the measurements of the different instruments.

Silly Putty® is much more viscous than any of the other fluids we tested, and we were able to characterize it in our Weissenberg rheogoniometer. (Our Weissenberg rheogoniometer had been modified for testing melts and very viscous materials only.) This permitted us to measure first normal stress differences as well as viscosities, although the shear rate range we were able to cover was only slightly more than one decade.

FLOW VISUALIZATION

There were two primary reasons for carrying out a flow visualization study. First, we felt that a symmetric radial flow with a stagnation point in the center of the plates would be a strong indication that the plates were parallel. Second, we wished to determine whether any secondary flows with path lines in the θ direction exist in fast squeezes, as had been observed in radial flows between fixed parallel plates (Laurencena and Williams, 1974).

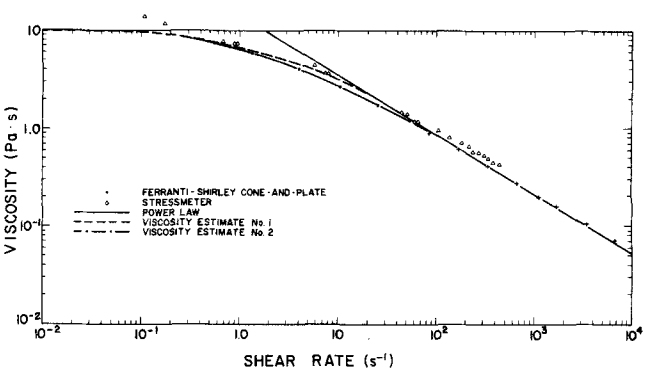

Fig. 4. Hydroxyethyl cellulose viscosity data. Falling ball viscometer tests gave a zero shear rate viscosity of 9.90 Pa · s.

Technique*

Since we wished to obtain only qualitative information about the radial flow pattern, our goal became that of obtaining a photograph of the flow path lines from beneath the lower plate. To do this, several modifications of the apparatus were necessary. The lower steel plate had to be replaced by a glass plate and the supporting structure redesigned to permit a clear optical path to the bottom of the plate. This meant eliminating the force transducer and the temperature control system from the equipment.

Small aluminum particles were suspended in the fluid at a high concentration to provide the light scattering points. During an experiment the shutter of the camera was left open, so that as the aluminum particles moved,

* Thanks are extended to Dr. Alberto Co for assisting with the photography in this study.

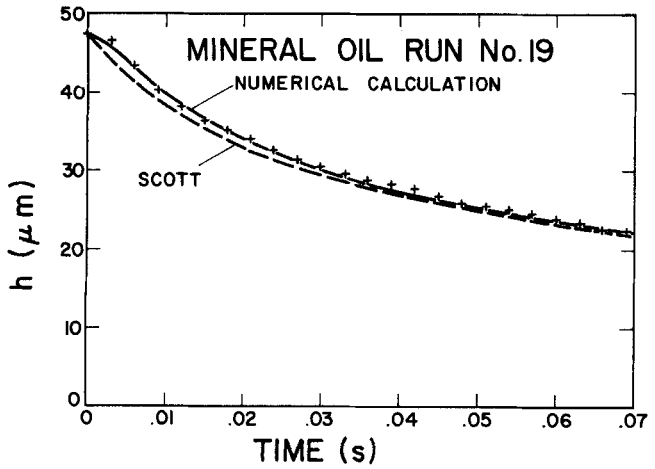

Fig. 5. Comparison of data taken on the mineral oil with the theory of Scott and with a numerical calculation which included both fluid and apparatus inertia. The numerical calculation also took into account the rise time of the current through the motor by using an expression for force given by

$$F = F_0\,[1 - \exp(-t/\beta)]$$

where β is the time constant for the current rise (in our case 2 ms). The crosses + represent experimental points. $F = 30.1$ N, $R = 0.635$ cm, $h_0 = 47.5$ μm.

light reflected from them left streaks on the film. Lighting was provided by a stroboscope, not because we wished to measure fluid velocities, but rather because the stroboscope could be automatically turned on and off at the beginning and end of each experiment by the same circuit that controlled the motor.

Results

The flow visualization photographs yielded no surprises; even in fairly fast experiments the flow was purely radial, with a stagnation point in the center of the plates. The ability of our flow visualization experiments to discriminate radial flows was tested by doing an experiment in which a broken magnet had been glued to the top plate. Path lines were clearly curved, and the center of the flow was not in the center of the plates.

INERTIA

Consideration must be given to both the effect of apparatus inertia and the effect of fluid inertia on our experimental results. Both would tend to slow the descent of the top plate. Apparatus inertia arises from the finite mass of the moving parts of the equipment. Fluid inertia arises from the mass of the fluid itself and is represented in fluid mechanics derivations by the inertial terms in the equations of motion. In this section we will develop an expression that can be used for estimating the magnitude of inertial effects and show that in all but a few of our fastest experiments these effects were small.

Apparatus Inertia

The effect of apparatus inertia can be taken into account in the Scott equation by replacing the left-hand side of Equation (2) with

$$F + 2M\ddot{h} \tag{7}$$

Fluid Inertia

Elkouh (1976) has recently carried out a perturbation analysis including fluid inertia for a power law fluid. He developed two different expressions, one using a momentum integral method and the other using an energy integral method. The two do not differ appreciably, so let us use the second one, which is given in his Equation (16) If we rewrite this equation, we obtain

$$F = F_{\text{inertialess}} + \left(\frac{C}{2}\right)\pi\rho R^4\left(\frac{\dot{h}}{h}\right)^2 - \left(\frac{B}{2}\right)\pi\rho R^4\left(\frac{\ddot{h}}{h}\right) \tag{8}$$

where $F_{\text{inertialess}}$ is given by Equation (2).

We note that this equation differs from one developed for Newtonian fluids (Ishizawa, 1966; Kuzma, 1967) only to the extent that

$$\begin{aligned} C/2 &\quad \text{differs from} \quad 15/56 \\ \text{and} & \\ B/2 &\quad \text{differs from} \quad 3/20 \end{aligned} \tag{9}$$

Interestingly, it appears that neither B nor C is a strong function of n, and that neither pair of terms compared above differ by more than 15%. The expression developed by Ishizawa and Kuzma has been compared with a numerical solution by Grimm (1976) and found to be in quite good agreement.

Current Rise Time

One additional effect on force that must be taken into account is the exponential rise time of the current through the motor to its steady state level. This can be done by using an expression for force given by

$$F = F_0\,[1 - \exp(-t/\beta)] \tag{10}$$

where β is the time constant for the current rise (in our case 2 ms).

Magnitude of Effects

If we combine Equations (2), (7), (8), and (10), we obtain

$$F_0\,[1 - \exp(-t/\beta)] + 2M\ddot{h} = \left(\frac{2n+1}{2n}\right)^n\left(\frac{\pi m R^{n+3}}{n+3}\right)\frac{(-\dot{h})^n}{h^{2n+1}} + \left(\frac{C}{2}\right)\pi\rho R^4\left(\frac{-\dot{h}}{h}\right)^2 - \left(\frac{B}{2}\right)\pi\rho R^4\left(\frac{\ddot{h}}{h}\right) \tag{11}$$

Appropriate initial conditions are

$$\begin{aligned} &\text{at} \quad t = 0 \quad h = h_0 \\ &\text{at} \quad t = 0 \quad \dot{h} = 0 \end{aligned} \tag{12}$$

We may apply the Runge-Kutta technique to this equation to obtain a numerical solution for $h(t)$. Figure 5 shows the results of such a calculation for our mineral oil. For this particular experiment, the rise time of the motor current was much more significant than the inertial effects. From a number of such calculations we have developed the rule of thumb that data points taken during the first 10 ms of an experiment should be discounted, as the effect of inertia is probably very significant during this period. Of course, for precise results, the complete numerical solution should be obtained for each given set of experimental conditions.

VISCOUS HEATING

A complete numerical solution of both the equation of motion using the power law and the energy equation has been given for squeezing flows by Booth and Hirst (1970*b*). Their method of solution follows that of Gould (1967), who solved the problem for a Newtonian liquid. The effect of both temperature and pressure on viscosity was included.

Booth and Hirst correlated their results in terms of two dimensionless groups

$$D = 2\delta/(\alpha\rho c) \tag{13}$$

and

$$J_s = \frac{3\alpha R m_0}{4h}\left[\frac{R(-\dot{h})}{h^2}\right]^n \tag{14}$$

If we evaluate these parameters for a typical set of experimental conditions, and compare them with the graph presented by Booth and Hirst, we find that the effect of viscous heating is negligible in our experiments.

Confirmation that viscous heating is unimportant is given by the experiments with the mineral oil and with the more viscous polybutene. If viscous heating had a significant effect, it would be expected to cause the plates to come together more quickly than predicted by the Scott equation, Equation (3). For the mineral oil, however, excellent agreement was found between the data and Equation (3). For the polybutene, the plates came together more slowly than predicted by the Scott equation in the faster squeezes, when viscous heating would be most important.

COMPRESSIBILITY

It is desirable to obtain an estimate of the impact of fluid compressibility on our results. A number of workers have presented theoretical developments in which compressibility is considered, but these have been primarily limited to ideal gases and sinusoidal oscillations of the top plate (Sadd and Stiffler, 1975; Langlois, 1962; also see an experimental study by Salbu, 1964). In the following development, we derive a perturbation solution about the parameter ϵ for a Newtonian fluid with a density given by

$$\frac{\rho}{\rho_a} = 1 + \epsilon\frac{(p - p_a)}{p_a} \tag{15}$$

The starting point for our derivation is the Reynolds equation for a compressible fluid (Langlois, 1964):

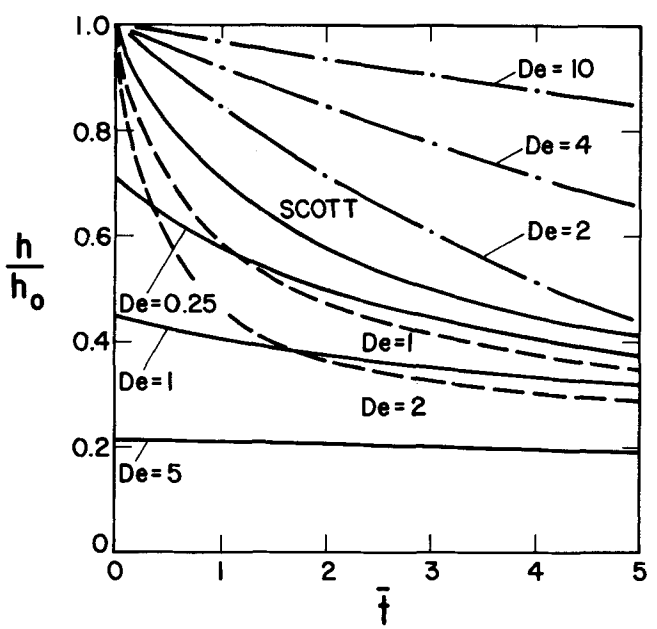

Fig. 6. Predictions of three different theories. Here we have plotted curves showing plate separation as a function of dimensionless time. Each theory predicts a family of curves that are dependent on the Deborah number $De = \lambda/t_{1/2}$ (Scott). For a Deborah number of zero, the theories of Tanner and of Brindley et al. reduce to the Scott equation. ——— Tanner (1965), $n = 1$. – – – – – – Brindley, Davies, and Walters (second-order fluid) (1976). ——·—— Parlato (1969), $R/h_0 = 50$.

$$\frac{1}{r}\frac{\partial}{\partial r}\left[rh^3\rho\left(\frac{\partial p}{\partial r}\right)\right] = 3\mu\frac{\partial(\rho h)}{\partial t} \tag{16}$$

If we substitute Equation (15) into Equation (16) and expand the pressure in a perturbation series about ϵ; that is

$$p = p_0 + p_1\epsilon + \ldots \tag{17}$$

we find after several steps that to first order in ϵ

$$F = \frac{3}{8}\pi\mu R^4\frac{(-\dot{h})}{h^3} + \frac{3}{16}\pi R^6\left(\frac{\mu\dot{h}}{h^3}\right)^2\left[\frac{h\ddot{h}}{(\dot{h})^2} - \frac{5}{2}\right]\frac{\epsilon}{p_a} \tag{18}$$

(valid for all plate motions)

This is the same as Equation (18) in Sadd and Stiffler's 1975 paper if ϵ is set equal to unity, as we perhaps might have anticipated since Equation (15) reduces to Boyle's law for ideal gases when $\epsilon = 1$. Their equation, then, is more general than it appears and is not limited to the sinusoidal plate motions for which it was derived.

Equation (18) can be solved for $h(t)$ using the Runge-Kutta numerical method. It was found that the effect of compressibility on our results was not significant for those liquids that did not contain gas bubbles.

RESULTS AND DISCUSSION

Nondimensionalization

Since we will be presenting a large amount of data, it is advantageous to present our results in terms of dimensionless variables that will bring data from widely different experimental conditions onto a single scale. We would like to plot our results in terms of h/h_0 vs. a dimensionless time $\bar{t}$. The Scott equation, Equation (3), has been found in previous studies to fit data for slow squeezes well, so let us use it to suggest an appropriate definition of $\bar{t}$. We will choose

$$\bar{t} = (h_0/h_{\text{Scott}})^2 - 1 \tag{19}$$

or

$$\bar{t} = [1 + (1 + 1/n)\, h_0^{1+1/n}\, kt]^{2n/(1+n)} \tag{20}$$

where k is given in Equation (4). With this definition for $\bar{t}$, a power law fluid will have a squeeze flow curve given by

$$h/h_0 = (1 + \bar{t})^{-1/2} \tag{21}$$

The variable $\bar{t}$ was chosen deliberately to give this curve, since the curve is similar to what is observed experimentally if one plots h/h_0 vs. t. Nonpower law fluids also retain a shape similar to what one sees when plotting h/h_0 vs. t if one instead plots h/h_0 vs. $\bar{t}$. For powers of n not equal to one, the time scale is distorted. Short times tend to be emphasized more, since the data near the end of an experiment will tend to be collapsed together. This can be seen by noting that for a given F, R, h_0, m, and n, Equation (20) is of the form

$$\bar{t} = (1 + at)^b - 1 \tag{22}$$

For n less than unity, b will be less than unity, and the time scale will be distorted.

Theoretical Predictions

It is useful at this point to put some of the theoretical developments discussed previously in terms of our dimensionless variables h/h_0 and $\bar{t}$. The resultant expressions can then be used to obtain the plot given in Figure 6.

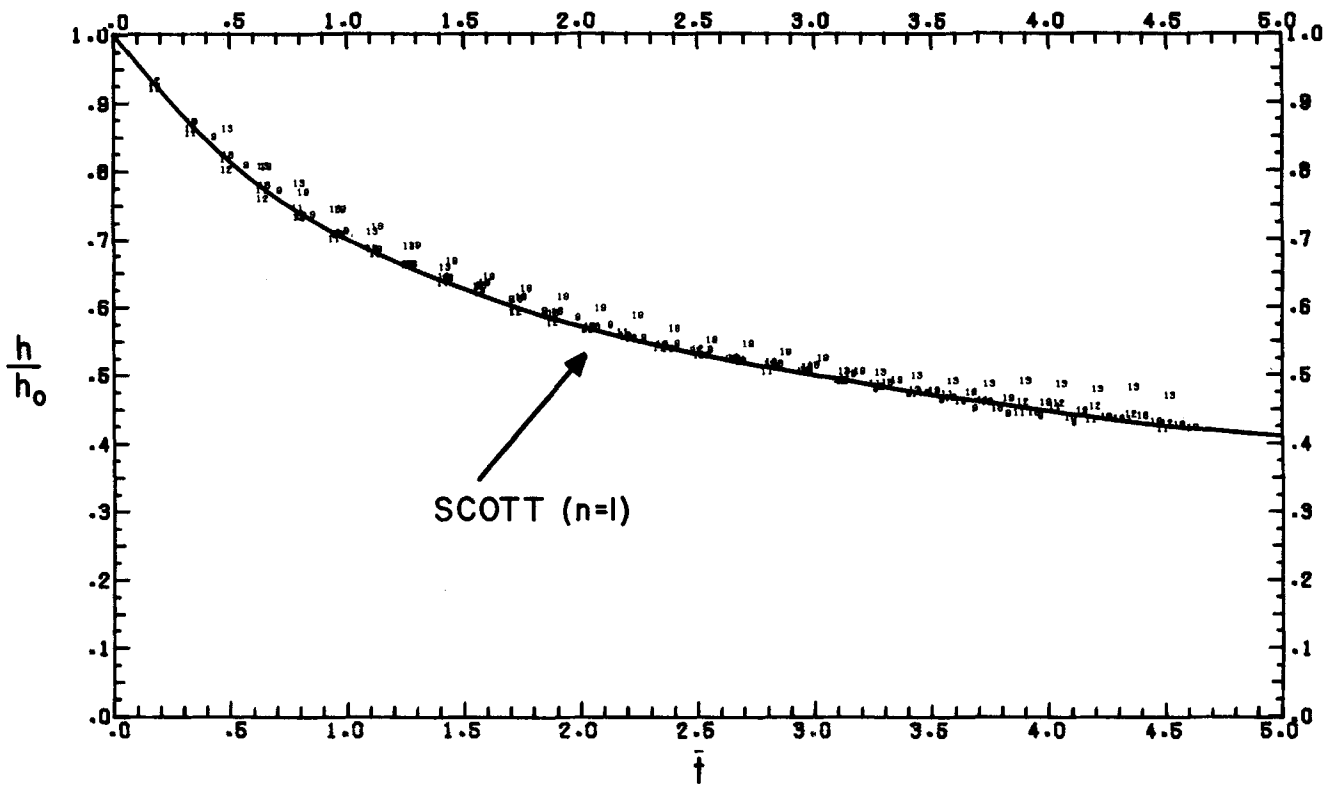

Fig. 7. Data taken on the mineral oil in terms of our dimensionless variables h/h_0 and $\bar{t}$. The number designating each data point refers to the run number assigned to that particular experiment.

Tanner (1965). Equation (15) in Tanner's paper can be rewritten as

$$\frac{h}{h_0} = \left[(1+\bar{t})^{2-n} + \frac{\lambda}{t_{1/2}\,(\text{Scott})}\left(\frac{2^{4-2n}-1}{3-2n}\right)\right]^{-1/(4-2n)} \quad (23)$$

where $t_{1/2}$(Scott) is the half time predicted by the Scott equation and is given by

$$t_{1/2}(\text{Scott}) = n\,K_n\left(\frac{\pi R^2 m}{F}\right)^{1/n}\left(\frac{R}{h_0}\right)^{1+1/n} \quad (24)$$

where

$$K_n = \left(\frac{2^{1+1/n}-1}{2n}\right)\left(\frac{2n+1}{n+1}\right)\left(\frac{1}{n+3}\right)^{1/n} \quad (25)$$

We see that a plot of h/h_0 vs. $\bar{t}$ will give a family of curves dependent on the parameters n and $\lambda/t_{1/2}$(Scott). Only curves for which $n = 1$ are included in Figure 6. Note that a step change in h at $t = 0$ is predicted by Equation (23).

Parlato (1969). Parlato's result can be written as

$$\frac{h}{h_0} = \exp\left\{-\left(\frac{\sqrt{\psi^2+8}-\psi}{12\lambda/t_{1/2}(\text{Scott})}\right)\bar{t}\right\} \quad (26)$$

where

$$\psi = \frac{16}{3}\left(\frac{h_0}{R}\right)^2\left(\frac{t_{1/2}(\text{Scott})}{\lambda}\right) - 1 \quad (27)$$

We see then that h/h_0 is an exponential function of $\bar{t}$, dependent on the two parameters R/h_0 and $\lambda/t_{1/2}$(Scott). If R/h_0 is large, however, $\psi = -1$, and only the parameter $\lambda/t_{1/2}$(Scott) is important. Only curves for which $R/h_0 = 50$ are included in Figure 6.

Kramer (1974). Since Kramer's results are based on a numerical development, we cannot cast them in terms of our dimensionless groups. A plot of his curves would, however, resemble the plot of Tanner's results given in Figure 6.

Leider and Bird (1974). Once again, some numerical work is necessary to obtain h/h_0 as a function of time. Leider and Bird's curves will, though, resemble those of Parlato.

Brindley, Davies, and Walters (1976). If we let

$$\lambda = -(9/10)[\alpha_2 - (3/2)\alpha_3]/\alpha_1 \quad (28)$$

in Equation (45) of their paper, we find that for a second-order fluid

$$\frac{h}{h_0} = (1+\bar{t})^{-1/2}\left\{1 + \frac{\lambda}{t_{1/2}(\text{Scott})}(1+\bar{t})\ln\left[(1+\bar{t})^{-1/2}\right]\right\} \quad (29)$$

Note that a plot of h/h_0 vs. $\bar{t}$ will yield a family of curves dependent on only the one parameter $\lambda/t_{1/2}$(Scott).

Experimental Results

Mineral Oil. One curve showing the behavior of the mineral oil has already been presented in Figure 5. We have plotted these data along with the data for the remainder of our tests in Figure 7 in terms of our dimensionless variables h/h_0 and $\bar{t}$. The individual data points are, in fact, numbers corresponding to the experimental run numbers. As expected, the data lie close to the Scott curve.

Coincidentally, in a number of additional experiments,

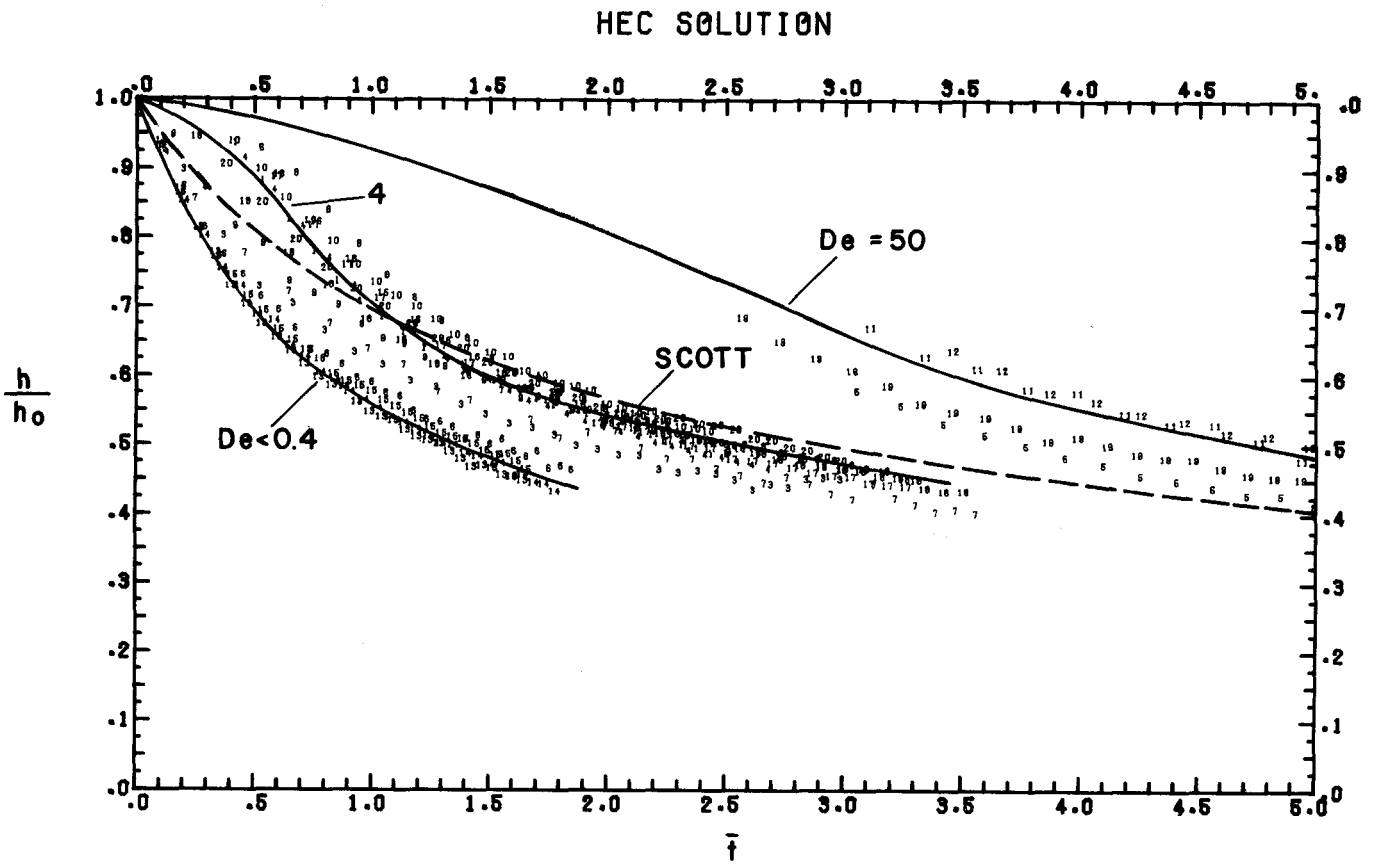

Fig. 8. Hydroxyethyl cellulose experimental data. Data taken during the first 10 ms of each experiment have been omitted, since they are probably greatly influenced by inertia. The Deborah number next to each curve is an average for several experimental runs close to that curve. $De = \lambda/t_{1/2}$ (Scott).

air bubbles were accidentally entrained in the liquid. The effect of the bubbles was to cause the top plate to descend more rapidly than predicted by Scott. This might be expected not only because the fluid was compressible, but also because the bubbles lowered the effective viscosity of the fluid.

The experiments on the mineral oil also allow us to estimate an overall error for the equipment. Taken together, they indicate that the experimental value of h will be within about $\pm$ 5% of the value calculated from Equation (3) for any given time. A note of caution needs to be sounded with regard to this error estimate, however. Small inaccuracies in the equipment will be amplified more for a fluid with a highly non-Newtonian viscosity than for a Newtonian fluid. The error band for a non-Newtonian fluid then could be larger than $\pm$ 5%.

Polybutene Oil. Over thirty experiments were performed on the polybutene oil. The data show a slight departure from the Scott prediction for the faster experiments but good agreement for the slower experiments. In the faster experiments, the plates did not come together as quickly as predicted by the Scott equation. Unfortunately, it is difficult to correlate these results with those on our other fluids, since no estimate of a fluid time constant can be made.

Hydroxyethyl Cellulose. Figure 8 gives a plot of the experimental data on the HEC. Each solid curve represents typical experimental data near it. We note that many of the experimental curves lie below the Scott prediction, although some of the experimental curves lie above the Scott prediction. The points above the line are presumably a manifestation of the elastic nature of the liquid, but those below are a bit more difficult to explain. An at least partially satisfactory explanation is that in these tests the shear rates present in the squeezing flow geometry

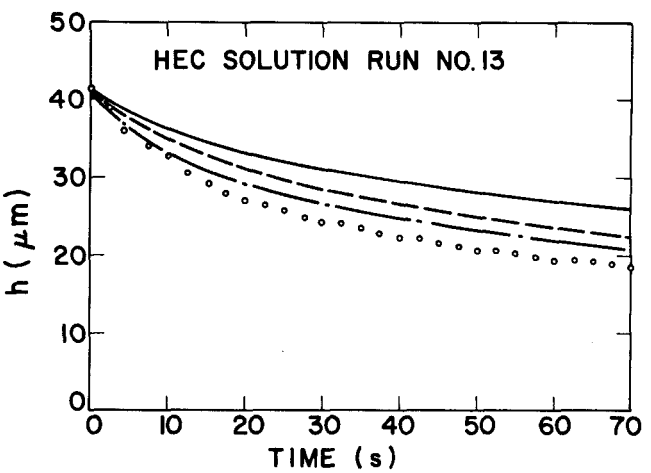

Fig. 9. Comparison of data taken on the HEC with curves predicted using the technique outlined by Brindley, Davies, and Walters (1976) for an arbitrary dependence of viscosity on shear rate. F = 18.6 N, R = 2.54 cm, h_0 = 41.6 μm. ——— Scott, Equation (3). - - - - - - prediction using viscosity estimate No. 1 (see Figure 4). —— · —— prediction using viscosity estimate No. 2 (see Figure 4). ○ = experimental data.

fell primarily below the power law region. We have used the method outlined by Brindley, Davies, and Walters (1976) to calculate plate separation for one of our experiments using the complete viscosity curve.* The results are shown in Figure 9. Since the viscosity of the HEC was not well known at low shear rates, we have used two different viscosity curves in the calculations. As can be seen in Figure 9, neither viscosity estimate gives a good

* Thanks are extended to Dr. J. Mansel Davies for carrying out the calculations associated with this study.

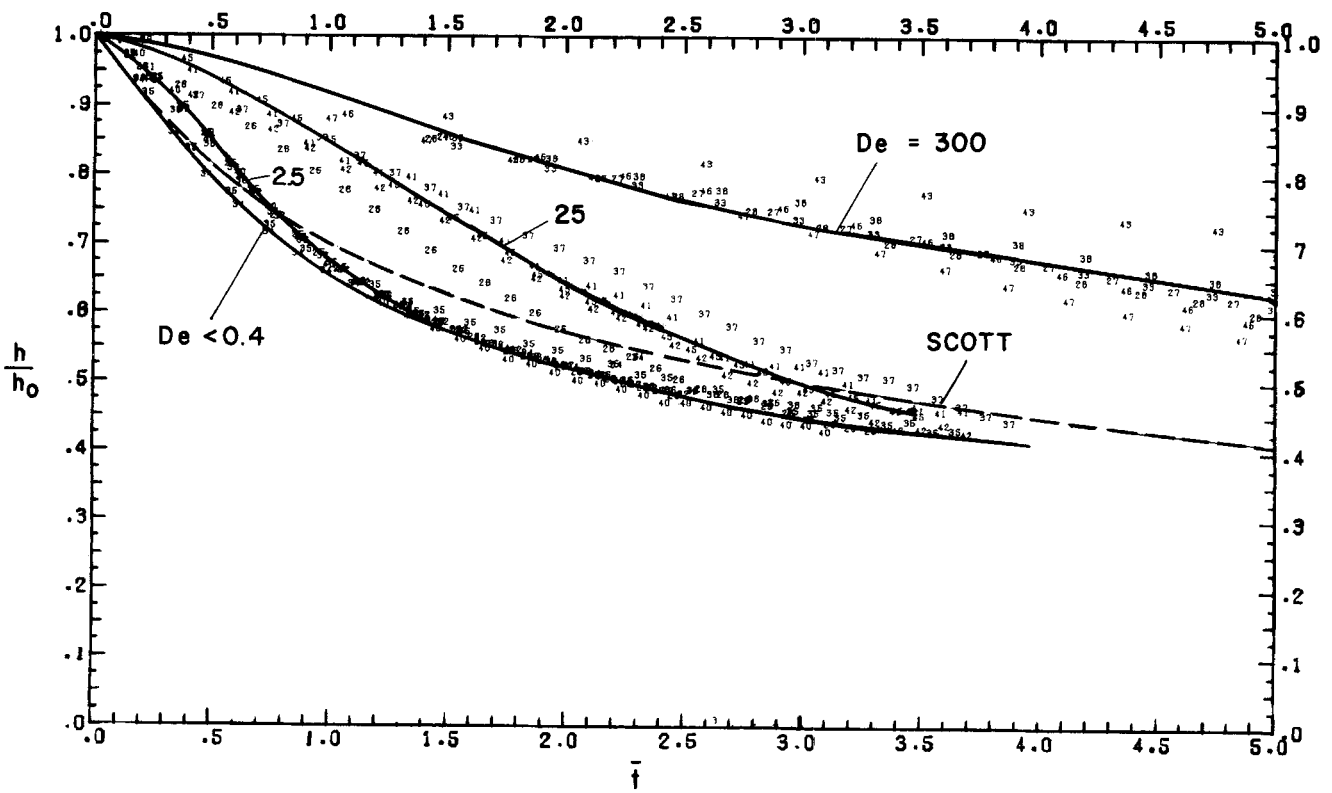

Fig. 10. Polyacrylamide experimental data. Data taken during the first 10 ms of each experiment have been omitted, since they are probably greatly influenced by inertia. The Deborah number next to each curve is an average for several experimental runs close to that curve. $De = \lambda/t_{1/2}$ (Scott).

fit to the experimental data, but the trend is in the right direction. Although some other influence might also cause data points to lie below the Scott prediction, we can say without hesitation that ignoring the zero shear rate viscosity region can result in large errors for slow squeezes.

Polyacrylamide. In Figure 10, the experimental data for the PA are presented. Here we see large deviations of the data from the Scott prediction due to elastic effects. Some data were taken with Deborah numbers as high as 4 000, showing even larger deviations than those present in Figure 10. These latter data extend off to the right of the graph in Figure 10, with no points being on scale because of our policy of omitting data taken during the first 10 ms of an experiment. We note from the figure that many of the experimental curves are S shaped, in striking contrast to the theoretical curves shown in Figure 6. Once again, some of the data for the slower squeezes lie below the Scott prediction, again probably because the zero shear rate viscosity region is neglected.

Silly Putty.® For the Silly Putty,® good agreement was found between the data for the slow squeezes and the Scott prediction, but in the fast squeezes the top plate descended more quickly than predicted by the Scott equation. A likely explanation for this is that the viscosity data taken by the Weissenberg Rheogoniometer do not extend to high enough shear rates to be in the power law region. In the fast experiments, then, the viscosity of the fluid is lower than predicted from rheogoniometer data, and as a result the top plate descends faster than predicted. The slow squeeze flow data are adequately modeled by the Scott equation, since the fluid viscosity at the low shear rates present in the gap is well described by the incorrect power law constants. This observation lends additional credence to the postulate that we need to use the complete viscosity vs. shear rate curve, and not just the power law viscosity, in modeling squeezing flow.

Polyethylene Oxide and Latex Suspension. The behavior of these two fluids was almost identical. Evidently, the effect of adding the latex particles to the PEO solution was only a minor one. This can be partially attributed to the fact that part of the PEO was adsorbed onto the particles, so that the total viscosity of the suspension remained relatively unchanged. In Figure 11 a plot of the data taken on the PEO is given. Once again, some of the data taken at higher Deborah numbers do not show on this scale. For the slower squeezes it can be seen that the experimental points lie below the Scott prediction. This is probably caused by a combination of the neglect of the zero shear rate viscosity and of the gas bubbles present in the solution. In the faster squeezes we see the same type of behavior observed with the PA. That is, the top plate does not descend as rapidly as predicted by Scott, and, moreover, a trace of plate separation as a function of time has an inflection point in it.

Correlation. For each of the given fluids, the amount the data departed from the Scott prediction, Equation (3), correlated well with the Deborah number, even for a quite wide ranging set of experimental conditions. This might have been expected on the basis of the dimensionless groups appearing in the theories discussed earlier in this section. The Deborah number has been defined here as $\lambda/t_{1/2}$(Scott), rather than $\lambda/t_{1/2}$(experiment). This follows the guide set by the theories and also permits a priori determination of the Deborah number using Equation (24).

A general dimensional analysis, however, reveals that two additional parameters must play some part. If we take as our variables h, t, R, F, h_0, m, n, and λ, and if there are three fundamental dimensions, the Buckingham Pi theorem states that we will have five dimensionless groups. These may be chosen to be

$$h/h_0, \quad \bar{t}, \quad De = \lambda/t_{1/2}(\text{Scott}), \quad R/h_0, \quad n \qquad (30)$$

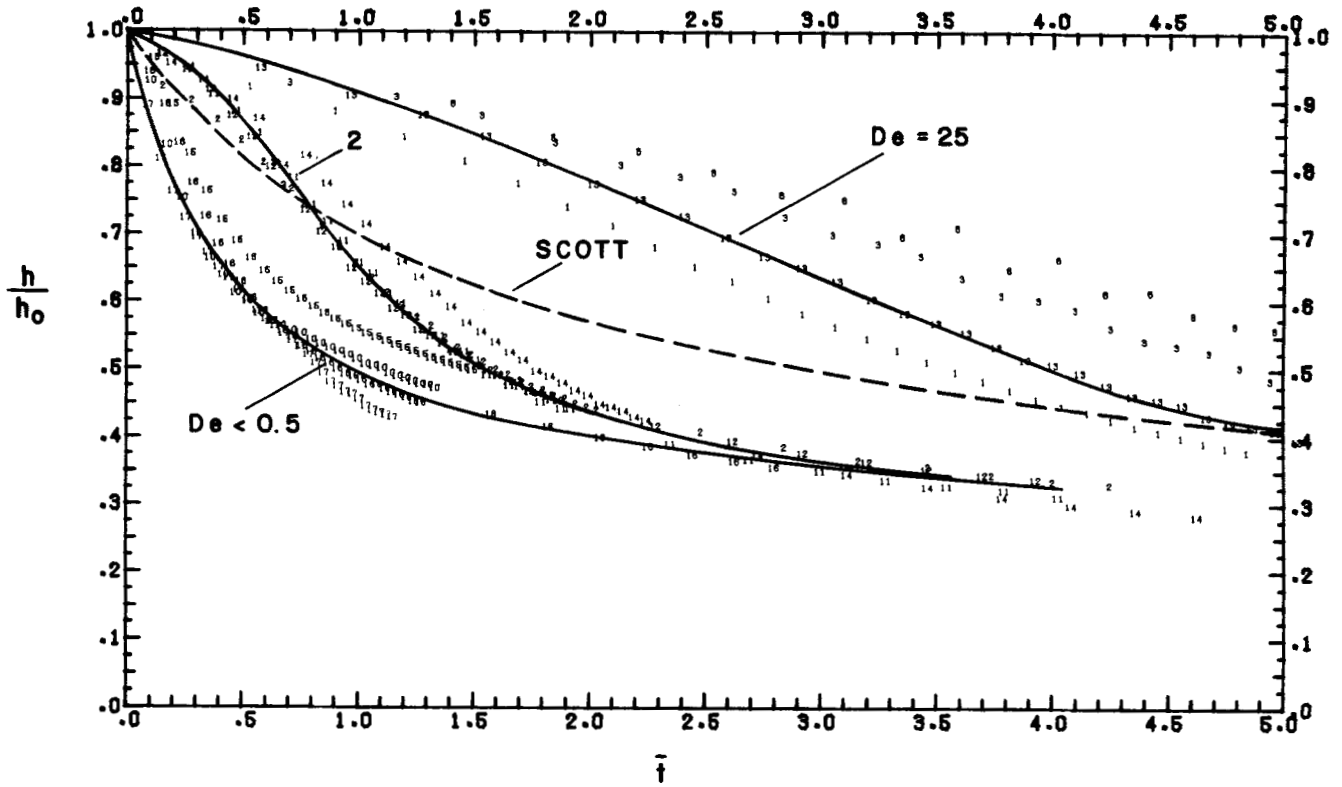

Fig. 11. Polyethylene oxide experimental data. The Deborah number [$De = \lambda/t_{1/2}$ (Scott)] next to each curve is an average for several experimental runs close to that curve. Data taken on the latex suspension were almost identical to those taken on the polyethylene oxide.

Note that in our correlations so far we have used only the first three of these. If the ratio R/h_0 is large, we might expect the effect of the ratio to be small. This evidently explains the relatively good correlations obtained for each fluid ignoring the parameter R/h_0.

A correlation that involves more than one fluid should also include the last parameter in (30), n. We present a general correlation, or master plot, in Figures 12 and 13 without using this parameter, however, since the values of n for our fluids did not differ greatly. In this plot we have taken the Scott equation as our low Deborah number asymptote. The correlation is not as good as the ones for each individual fluid and should be used only semiquantitatively.

Comparison of the general correlation in Figure 13 with the theoretical curves of Figure 6 shows that none of the theories is capable of describing the experimental results for the polymer solutions well. The theories of Tanner (1965), Kramer (1974), and Brindley, Davies, and Walters (for the second-order fluid) (1976) predict exactly the opposite trend with Deborah number to that observed experimentally. The theories of Parlato (1969) and of Leider and Bird (1974) do not show the S shape characteristic of many of the experimental curves, although they do predict the correct trend with Deborah number.

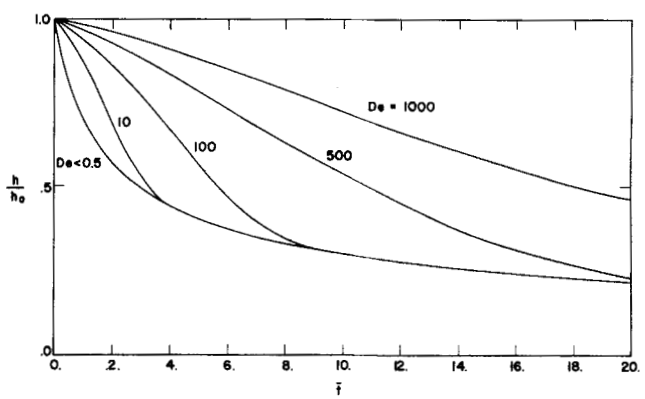

Fig. 12. Correlation of data for the polymer solutions tested. We have taken the Scott curve as the low Deborah number asymptote. This assumes that the zero shear rate viscosity region is small.

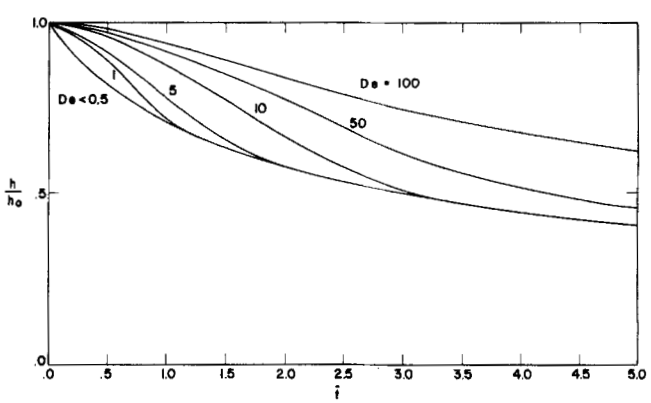

Fig. 13. Correlation shown in Figure 12, on an expanded scale.

ACKNOWLEDGMENT

Financial support for this work was obtained from the National Science Foundation (NSF) through Grants No. GK-24749 and ENG 75-01092, from the Wisconsin Alumni Research Fund of the University of Wisconsin and from Texaco Oil Company. Special thanks are owed to Mr. Alberto Co for assisting with the flow visualization, Dr. J. Mansel Davies for carrying out the numerical calculations leading to Figure 9, and to Mr. Ron McCabe and Mr. Al Hanson for invaluable aid in the construction of the experimental equip-

ment. The author has also profited greatly from conversations with Professor Arthur S. Lodge, Dr. Philip J. Leider, and other members of the Rheology Research Center at the University of Wisconsin. Finally, thanks must be extended to the author's major professor, Professor R. Byron Bird, without whose guidance and inspiration this work could not have been accomplished.

NOTATION

a = constant [see Equation (22)], s^{-1}
b = constant [see Equation (22)], dimensionless
B = coefficient, function of n only, dimensionless
c = specific heat of fluid, N · m/(kg · °K)
C = coefficient, function of n only, dimensionless
D = dimensionless group defined in Equation (13)
De = Deborah number, $\lambda/t_{1/2}$, dimensionless
F = force applied to the plastometer plates, N; F_0 = steady state constant force
h = half of the distance, or gap, between the two plastometer plates, m; h_0 = at time $t = 0$; h_0' = measured; h_{Scott} = as predicted by the Scott equation
$\dot{h}$ = $\partial h/\partial t$, m/s
J_s = dimensionless group defined in Equation (14)
k = variable defined in Equation (4), $[m^{(1+1/n)} \cdot s]^{-1}$
K_n = coefficient defined in Equation (25), function of n only, dimensionless
m = power law parameter defined in Equation (1), Pa · s^n; m_0 = at temperature T_0
m' = power law parameter for first normal stress difference (that is, $\tau_{11} - \tau_{22} = -m'\dot{\gamma}^{n'}$), Pa · $s^{n'}$
M = mass of all moving parts of the experimental apparatus, kg
n = exponent in power law defined in Equation (1), dimensionless
n' = exponent in power law for first normal stress difference (that is, $\tau_{11} - \tau_{22} = -m'\dot{\gamma}^{n'}$), dimensionless
p = pressure, Pa; p_a = atmospheric pressure; p_0, p_1 = pressure components defined in perturbation series of Equation (17)
r = coordinate direction defined in Figure 1
R = radius of the circular plastometer plates, m
t = time, s
$\bar{t}$ = dimensionless time, defined in Equation (19)
$t_{1/2}$ = half time, defined in Figure 2, s; $t_{1/2}$(Scott) = as predicted by the Scott equation, Equation (24)
T = temperature, °K
v_r = fluid velocity in the r direction, m/s
v_z = fluid velocity in the z direction, m/s
v_θ = fluid velocity in the θ direction, m/s
z = coordinate direction defined in Figure 1

Greek Letters

$\alpha = -\frac{1}{m}\left(\frac{\partial m}{\partial p}\right)_T$, m^2/N

$\alpha_1, \alpha_2, \alpha_3$ = second-order fluid constants

$$\underline{\tau} = -\alpha_1\underline{\dot{\gamma}} - \alpha_2\left[\frac{\partial}{\partial t}\underline{\dot{\gamma}} + \{\mathbf{v}\cdot\nabla\underline{\dot{\gamma}}\} + \frac{1}{2}\left(\{\underline{\omega}\cdot\underline{\dot{\gamma}}\} - \{\underline{\dot{\gamma}}\cdot\underline{\omega}\}\right)\right] - (\alpha_2+\alpha_3)\,(\underline{\dot{\gamma}}\cdot\underline{\dot{\gamma}})$$

α_1, Pa · s
α_2, α_3, Pa · s^2

β = time constant for current rise, s
$\dot{\gamma}$ = shear rate, $\sqrt{\frac{1}{2}(\underline{\dot{\gamma}}:\underline{\dot{\gamma}})}$, s^{-1}
$\underline{\dot{\gamma}}$ = rate of deformation tensor, $\nabla\mathbf{v} + (\nabla\mathbf{v})^\dagger$, s^{-1}
$\delta = -\frac{1}{m}\left(\frac{\partial m}{\partial T}\right)_p$, $(°K)^{-1}$
ϵ = perturbation parameter defined in Equation (15), dimensionless
η = apparent viscosity, $\tau_{12}/\dot{\gamma}$, Pa · s; η_0 = zero shear rate viscosity
θ = coordinate direction
λ = time constant of fluid, s
μ = viscosity, Pa · s
ρ = density, Kg/m^3; ρ_a = atmospheric
$\underline{\tau}$ = extra stress tensor, Pa; we have used the sign convention of Bird, Armstrong, and Hassager (1977)
ψ = variable defined by Equation (27), dimensionless
$\underline{\omega}$ = vorticity tensor, $\nabla\mathbf{v} - (\nabla\mathbf{v})^\dagger$, s^{-1}

LITERATURE CITED

Binding, D. M., J. M. Davies, and K. Walters, "Elastico-Viscous Squeeze Films: Part 2. Superimposed Rotation," *J.N.N.F.M.*, **1**, 259 (1976).

Binding, D. M., and K. Walters, "Elastico-Viscous Squeeze Films: Part 3: The Torsional Balance Rheometer, *ibid.*, 277 (1976).

Bird, R. B., R. C. Armstrong, and O. Hassager, *Dynamics of Polymeric Liquids*, Vol. 1, *Fluid Mechanics*, pp. 223-226, Wiley, New York (1977).

Booth, M. J., and W. Hirst, "The Rheology of Oils During Impact: I. Mineral Oils," *Proc. Roy. Soc. London*, **A316**, 391 (1970*a*).

———, "The Rheology of Oils During Impact: Part II. Silicone Fluids," *ibid.*, 415 (1970*b*).

Brindley, G., J. M. Davies, and K. Walters, "Elastico-Viscous Squeeze Films. Part 1," *J.N.N.F.M.*, **1**, 19 (1976). (One line after Eq. 45, change "less" to "greater"; the solution given in Eq. 41 is not exact but rather a result of a perturbation analysis.)

Co, A., and R. B. Bird, "Analysis of Squeezing Flow Between Parallel Disks Using the Goddard-Miller Model," *Rheology Research Center Rept. No. 31*, Univ. Wisc., Madison (1974).

Dienes, G. J., "Viscoelastic Properties of Thermoplastics at Elevated Temperatures," *J. Colloid Sci.*, **2**, 131 (1947).

———, and H. F. Klemm, "Theory and Application of the Parallel Plate Plastometer," *J. Appl. Phys.*, **17**, 458 (1946).

Dodge, J. S., M. E. Woods, and J. M. Krieger, *J. Paint Tech.*, **42**, 541 (1970).

Elkouh, A. F., "Fluid Inertia Effects in Non-Newtonian Squeeze Films," *J. Lub. Tech.*, Paper No. 76—Lub-J (1976).

Freeman, G. C., *Silicones*, pp. 94-95, Iliffe Books, Ltd., London, England (1962).

Gould, P., "Parallel Surface Squeeze Films: The Effect of the Variation of Viscosity with Temperature and Pressure," *J. Lub. Tech., Trans. ASME*, **89**, 375 (1967).

Greenspan, D., *Discrete Numerical Methods in Physics and Engineering*, Academic Press, New York (1974).

Grimm, R. J., "Squeezing Flows of Newtonian Liquid Films," *Appl. Sci. Res.*, **32**, 149 (1976).

———, "Squeezing Flows of Polymeric Liquids," Ph.D. thesis, Univ. Wisc., Madison (1977).

Higashitani, K., and A. S. Lodge, "Hole Pressure Error Measurements in Pressure-generated Shear Flow," *Trans. Soc. Rheol.*, **19**, 307 (1975).

Hirst, W., and M. G. Lewis, "The Rheology of Oils During Impact: III. Elastic Behavior," *Proc. Roy. Soc. London*, **A334**, 1 (1973).

Ishizawa, S., "The Unsteady Laminar Flow Between Two Parallel Discs with Arbitrarily Varying Gap Width," *Bulletin of J.S.M.E.*, **9**, 533 (1966).

Kramer, J. M., "Large Deformations of Viscoelastic Squeeze Films," *Appl. Sci. Res.*, **30**, 1 (1974).

Kuzma, D. C., "Fluid Inertia Effects in Squeeze Films," *ibid.*, **18**, 15 (1967).

Langlois, W. E., "Isothermal Squeeze Films," *Quart. Appl. Math.*, **20**, 131 (1962).

———, *Slow Viscous Flow*, MacMillan (1964).

Laurencena, B. R., and M. C. Williams, "Radial Flow of Non-Newtonian Fluids Between Parallel Plates," *Trans. Soc. Rheol.*, **18**, 331 (1974).
Leider, P. J., "Squeezing Flow Between Parallel Disks" II. Experimental Results," *Ind. Eng. Chem. Fundamentals*, **13**, 342 (1974).
———, and R. B. Bird, "Squeezing Flow Between Parallel Disks: I. Theoretical Analysis," *ibid.*, 336 (1974).
Metzner, A. B., "Extensional Primary Field Approximations for Viscoelastic Media," *Rheol. Acta.*, **10**, 434 (1971).
Na, T. Y., "The Non-Newtonian Squeeze Film," *J. Basic Eng., Trans. ASME*, **88**, 687 (1966).
Novotny, E. J., Jr., and R. Eckert, "Direct Measurement of Hole Error For Viscoelastic Fluids in Flow Between Infinite Parallel Plates," *Trans. Soc. Rheol.*, **17**, 227 (1973).
Parlato, P., M. S. thesis, Univ. Del., Newark (1969).
Riddle, M. J., C. Narvaez, and R. B. Bird, "Interactions Between Two Spheres Falling Along Their Line of Centers in a Viscoelastic Fluid," *J.N.N.F.M.*, **2**, 23 (1977).
Sadd, M. H., and A. K. Stiffler, "Squeeze Film Dampers: Amplitude Effects at Low Squeeze Numbers," *J. Eng. Ind.*, **97**, 1366 (1975).
Salbu, E. O. J., "Compressible Squeeze Films and Squeeze Bearings," *J. Basic Eng.*, **86**, 355 (1964).
Scott, J. R., "Theory and Application of the Parallel-Plate Plastimeter," *Trans. I.R.I.*, **7**, 169 (1931).
Stefan, J., "Versuche über die scheinbare Adhäsion," *Akad. Wiss. Math. Natur., Wien*, **69**, Part 2, 713 (1874).
Sutterby, J. L., "Falling Sphere Viscometry: I. Wall and Inertial Corrections to Stoke's Law in Long Tubes," *Trans. Soc. Rheol.*, **17**, 559 (1973).
Tanner, R. I., "Some Illustrative Problems in the Flow of Viscoelastic Non-Newtonian Lubricants," *ASLE Trans.*, **8**, 179 (1965).
Turian, R. M., "Thermal Phenomena and Non-Newtonian Viscometry," Ph.D. thesis, p. 112, Univ. Wisc., Madison (1964).
Williams, G., and R. I. Tanner, "Effects of Combined Shearing and Stretching in Viscoelastic Lubrication," *J. Lub. Tech., Trans. ASME*, **92**, 216 (1970).

Manuscript received June 29, 1977; revision received December 8, and accepted December 16, 1977.

Liquid Distribution in Trickle-Bed Reactors

MORDECHAY HERSKOWITZ
and
J. M. SMITH
University of California
Davis, California 95616

Part I. Flow Measurements

Radial liquid distribution was measured for concurrent downflow of air and water through beds packed with catalyst particles. The experimental results can be predicted by a theory involving two parameters, a spreading factor S and wall factor *f*. Criteria are presented for predicting operating conditions (particle size and shape and tube diameter) for which the equilibrium distribution will be uniform and packed-bed depth required to attain equilibrium liquid distribution.

SCOPE

The effect of maldistribution of liquid in trickle beds has been a worrisome and unknown factor, both from the standpoint of the performance of commercial scale reactors (Ross, 1965) and interpretation of data from laboratory reactors (Satterfield, 1975; Levec and Smith, 1976). The extensive studies of liquid distribution in countercurrent flow absorption columns, summarized by Onda et al. (1973), indicated reasonably uniform flow in the central section of the packed column but excessive flow at the wall. The significant variables were distribution of the feed liquid, tvpe and size of the packing, column diameter, gas and liquid flow rates, and some physical properties.

It is expected that the same variables would be involved in the cocurrent downflow of gas and liquid in trickle beds. However, flow rates are substantially less, and the packing units, catalyst particles, are normally smaller and of different shape.

Quantitative experimental data for trickle beds appear to be limited to the papers of Prchlik et al. (1973, 1975*a*, *b*) and Specchia (1974). Their measurements were made for the pellets 0.64 to 0.98 cm in size (shape unknown) and without gas flow. The results were correlated with a diffusion type of equation involving three adjustable parameters. Unfortunately, most of the experimental data were not published in sufficient detail to be useful for evaluation purposes.

The objective of our work was twofold. We wanted to develop a method of predicting the radial distribution applicable for the gas continuous or trickling flow regime, as characterized by Charpentier (1976). This regime includes the range of gas and liquid flow rates normally encountered in trickle-bed reactors. We also wanted to measure as carefully as possible flow distributions which would be useful for evaluating our theory and others. Accordingly, data were obtained for fourteen catalyst particles of different size (0.26 to 1.1 cm), shape (granular, spherical, cylindri-